

Two-neutrino and neutrinoless double beta decay in the shell model

Luigi Coraggio

Istituto Nazionale di Fisica Nucleare - Sezione di Napoli

June 28th, 2019

Sala Polifunzionale, Marciana Marina



Acknowledgements

- A. Gargano (INFN-NA)
- N. Itaco (UNICAMPANIA and INFN-NA)
- R. Mancino (UNICAMPANIA and INFN-NA)
- F. Nowacki (IPHC Strasbourg and UNICAMPANIA)
- L. C. (INFN-NA)

- The neutrinoless double- β decay
- The calculation of the nuclear matrix element (NME) of $0\nu\beta\beta$ decay
- The realistic nuclear shell model (RSM)
- Present work:
 - Testing the RSM: calculation of the GT strengths and the nuclear matrix element of $2\nu\beta\beta$ decay
 - RSM calculation of $0\nu\beta\beta$ nuclear matrix element $M^{0\nu}$ and comparison with other SM results
 - Perturbative properties of the $0\nu\beta\beta$ effective operator
 - Evaluation of the $M^{0\nu}$
- Outlook

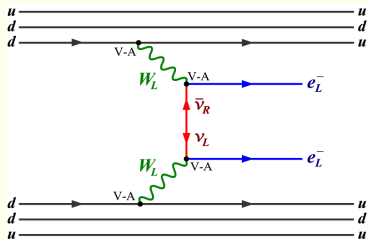
The detection of the $0\nu\beta\beta$ decay is nowadays one of the main targets in many laboratories all around the world, triggered by the search of "new physics" beyond the Standard Model.

- Its detection
 - would correspond to a violation of the conservation of the lepton number,
 - may provide more informations on the nature of the neutrinos (the neutrino as a Majorana particle, determination of its effective mass, ..).

The neutrinoless double β -decay

The inverse of the $0\nu\beta\beta$ -decay half-life is proportional to the squared nuclear matrix element $M^{0\nu}$.

This property evidences the relevance to calculate $M^{0\nu}$



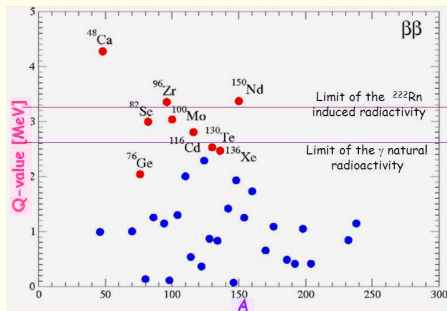
$$\left[T_{1/2}^{0\nu}\right]^{-1} = G^{0\nu} \left|M^{0\nu}\right|^2 \langle m_\nu \rangle^2$$

- $G^{0\nu}$ is the so-called phase-space factor, which can be accurately evaluated by atomic physics calculations;
- $\langle m_\nu \rangle = \left| \sum_k m_k U_{ek}^2 \right|$ effective mass of the Majorana neutrino (light-neutrino exchange)

The detection of the $0\nu\beta\beta$ -decay

It is necessary to locate the nuclei that are the best candidates to detect the $0\nu\beta\beta$ -decay

- The main factors to be taken into account are:
 - the Q -value;
 - the phase-space factor $G^{0\nu}$;
 - the isotopic abundance

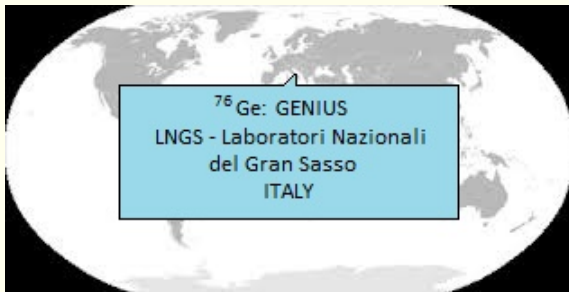


- First group: ^{76}Ge , ^{130}Te , and ^{136}Xe .
- Second group: ^{82}Se , ^{100}Mo , and ^{116}Cd .
- Third group: ^{48}Ca , ^{96}Zr , and ^{150}Nd .

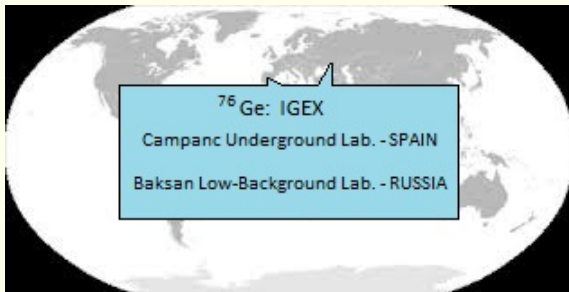
Our aim is to compute the $0\nu\beta\beta$ -decay NME for ^{48}Ca , ^{76}Ge , ^{82}Se , ^{130}Te , and ^{136}Xe .



Our aim is to compute the $0\nu\beta\beta$ -decay NME for ^{48}Ca , ^{76}Ge , ^{82}Se , ^{130}Te , and ^{136}Xe .



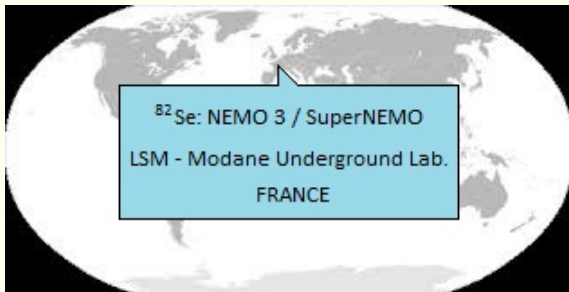
Our aim is to compute the $0\nu\beta\beta$ -decay NME for ^{48}Ca , ^{76}Ge , ^{82}Se , ^{130}Te , and ^{136}Xe .



Our aim is to compute the $0\nu\beta\beta$ -decay NME for ^{48}Ca , ^{76}Ge , ^{82}Se , ^{130}Te , and ^{136}Xe .



Our aim is to compute the $0\nu\beta\beta$ -decay NME for ^{48}Ca , ^{76}Ge , ^{82}Se , ^{130}Te , and ^{136}Xe .



Our aim is to compute the $0\nu\beta\beta$ -decay NME for ^{48}Ca , ^{76}Ge , ^{82}Se , ^{130}Te , and ^{136}Xe .



Our aim is to compute the $0\nu\beta\beta$ -decay NME for ^{48}Ca , ^{76}Ge , ^{82}Se , ^{130}Te , and ^{136}Xe .



Our aim is to compute the $0\nu\beta\beta$ -decay NME for ^{48}Ca , ^{76}Ge , ^{82}Se , ^{130}Te , and ^{136}Xe .



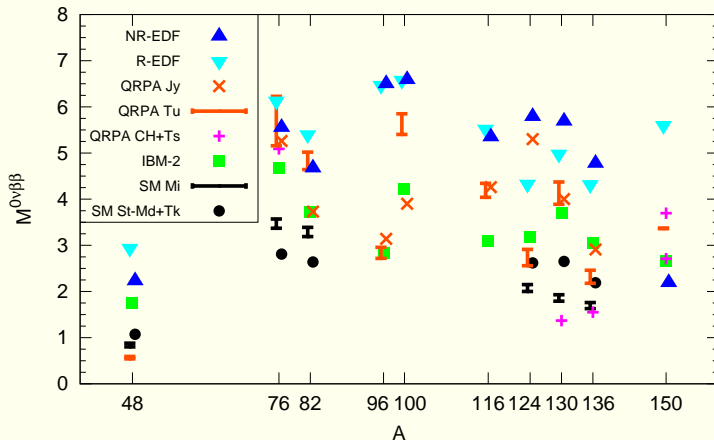
The calculation of the NME

To describe the nuclear properties detected in the experiments, one needs to resort to nuclear structure models.

- Every model is characterized by a certain number of parameters.
- The calculated value of the **NME** may depend upon the chosen nuclear structure model.

All models may present advantages and/or shortcomings to calculate the **NME**

Nuclear structure calculations



- The spread of nuclear structure calculations evidences inconsistencies among results obtained with different models

The renormalization of g_A, g_V

There are some arguments to employ $g_A^{\text{eff}}, g_V^{\text{eff}}$.
Effective coupling constants are necessary to take into account:

- the short-range correlations excluded to soften the NN force, when starting from realistic potentials;
- the degrees of freedom that have been excluded because of the truncation of the Hilbert space;
- contributions to the free values of g_A, g_V from meson exchange currents.

In this study we tackle the first two issues deriving effective-decay operators by way of the many-body perturbation theory

- H. Q. Song, H. F. Wu, T. T. S. Kuo, *Phys. Rev. C* **40**, 2260 (1989)
- A. Staudt, T. T. S. Kuo, H. V. Klapdor-Kleingrothaus, *Phys. Rev. C* **46**, 871 (1992)
- J. D. Holt and J. Engel, *Phys. Rev. C* **87**, 064315 (2013)

Effective shell-model hamiltonian

The shell-model hamiltonian has to take into account in an **effective way** all the degrees of freedom not explicitly considered

Two alternative approaches

- phenomenological
- microscopic

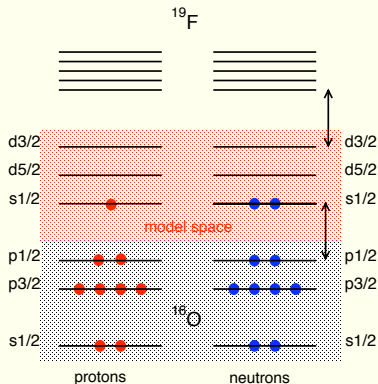
$$V_{NN} (+ V_{NNN}) \Rightarrow \text{many-body theory} \Rightarrow H_{\text{eff}}$$

Definition

The eigenvalues of H_{eff} belong to the set of eigenvalues of the full nuclear hamiltonian.

This may be provided by a **similarity transformation** Ω of the full Hilbert-space hamiltonian H

An example: ^{19}F



- 9 protons & 10 neutrons interacting
- spherically symmetric mean field (e.g. harmonic oscillator)
- 1 valence proton & 2 valence neutrons interacting in a truncated model space

The degrees of freedom of the core nucleons and the excitations of the valence ones above the model space are not considered explicitly.

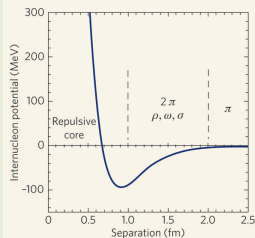
Workflow for a realistic shell-model calculation

- 1 Choose a realistic NN potential (NNN)
- 2 Renormalize its short range correlations
- 3 Identify the model space better tailored to study the physics problem
- 4 Derive the effective shell-model hamiltonian and consistently effective transition operators, by way of the many-body perturbation theory
- 5 Calculate the observables (energies, e.m. transition probabilities, β -decay amplitudes...), using only theoretical SP energies, two-body matrix elements, and effective operators.

Realistic nucleon-nucleon potential: V_{NN}

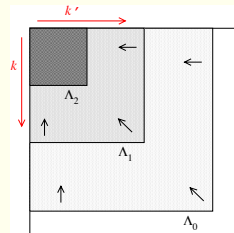
Several realistic potentials $\chi^2/datum \simeq 1$:
[CD-Bonn](#), Argonne V18, Nijmegen, ...

Strong short-range repulsion



How to handle the short-range repulsion ?

- Brueckner G matrix
- EFT inspired approaches
 - $V_{\text{low-}k}$, our chosen cutoff:
 $\Lambda = 2.6 \text{ fm}^{-1}$
 - SRG



The shell-model effective hamiltonian

We start from the many-body hamiltonian H defined in the full Hilbert space:

$$H = H_0 + H_1 = \sum_{i=1}^A (T_i + U_i) + \sum_{i < j} (V_{ij}^{NN} - U_i)$$

$$\left(\begin{array}{c|c} PHP & PHQ \\ \hline QHP & QHQ \end{array} \right) \xRightarrow{QHP=0} \left(\begin{array}{c|c} P\mathcal{H}P & P\mathcal{H}Q \\ \hline 0 & Q\mathcal{H}Q \end{array} \right)$$

$\mathcal{H} = \Omega^{-1} H \Omega$

$$H_{\text{eff}} = P\mathcal{H}P$$

Suzuki & Lee $\Rightarrow \Omega = e^{\omega}$ with $\omega = \left(\begin{array}{c|c} 0 & 0 \\ \hline Q\omega P & 0 \end{array} \right)$

$$H_1^{\text{eff}}(\omega) = PH_1P + PH_1Q \frac{1}{\epsilon - QHQ} QH_1P - \\ - PH_1Q \frac{1}{\epsilon - QHQ} \omega H_1^{\text{eff}}(\omega)$$

The perturbative approach to the shell-model H^{eff}

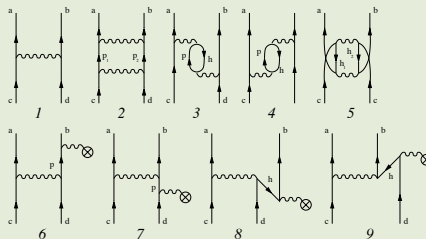
The \hat{Q} -box vertex function

$$\hat{Q}(\epsilon) = PH_1P + PH_1Q \frac{1}{\epsilon - QH_0Q} QH_1P$$

Exact calculation of the \hat{Q} -box is computationally prohibitive for many-body system \Rightarrow we perform a perturbative expansion

$$\frac{1}{\epsilon - QH_0Q} = \sum_{n=0}^{\infty} \frac{(QH_1Q)^n}{(\epsilon - QH_0Q)^{n+1}}$$

The diagrammatic expansion of the \hat{Q} -box



Effective operators for decay amplitudes

- ψ_α indicates eigenstates of the full hamiltonian H corresponding to eigenvalues E_α
- ϕ_α indicates the eigenvectors obtained diagonalizing H_{eff} in the reduced model space P and corresponding to the same eigenvalues E_α

$$\Rightarrow |\phi_\alpha\rangle = P |\psi_\alpha\rangle$$

Obviously, for any decay-operator Θ :

$$\langle \phi_\alpha | \Theta | \phi_\beta \rangle \neq \langle \psi_\alpha | \Theta | \psi_\beta \rangle$$

We then require an effective operator Θ_{eff} defined as follows

$$\Theta_{\text{eff}} = \sum_{\alpha\beta} |\phi_\alpha\rangle \langle \psi_\alpha | \Theta | \psi_\beta \rangle \langle \phi_\beta |$$

Consequently, the matrix elements of Θ_{eff} are

$$\langle \phi_\alpha | \Theta_{\text{eff}} | \phi_\beta \rangle = \langle \psi_\alpha | \Theta | \psi_\beta \rangle$$

The shell-model effective operators

Any shell-model effective operator may be derived consistently with the \hat{Q} -box-plus-folded-diagram approach to H_{eff}

It has been demonstrated that, for any bare operator Θ , a non-Hermitian effective operator Θ_{eff} can be written in the following form:

$$\Theta_{\text{eff}} = (P + \hat{Q}_1 + \hat{Q}_1 \hat{Q}_1 + \hat{Q}_2 \hat{Q}_1 + \hat{Q}_1 \hat{Q}_2 + \cdots)(\chi_0 + \chi_1 + \chi_2 + \cdots),$$

where

$$\hat{Q}_m = \frac{1}{m!} \left. \frac{d^m \hat{Q}(\epsilon)}{d\epsilon^m} \right|_{\epsilon=\epsilon_0},$$

ϵ_0 being the model-space eigenvalue of the unperturbed hamiltonian H_0

*K. Suzuki and R. Okamoto, Prog. Theor. Phys. **93**, 905 (1995)*

The shell-model effective operators

The χ_n operators are defined as follows:

$$\begin{aligned}\chi_0 &= (\hat{\Theta}_0 + h.c.) + \Theta_{00} , \\ \chi_1 &= (\hat{\Theta}_1 \hat{Q} + h.c.) + (\hat{\Theta}_{01} \hat{Q} + h.c.) , \\ \chi_2 &= (\hat{\Theta}_1 \hat{Q}_1 \hat{Q} + h.c.) + (\hat{\Theta}_2 \hat{Q} \hat{Q} + h.c.) + \\ &\quad (\hat{\Theta}_{02} \hat{Q} \hat{Q} + h.c.) + \hat{Q} \hat{\Theta}_{11} \hat{Q} , \\ &\quad \dots\end{aligned}$$

and

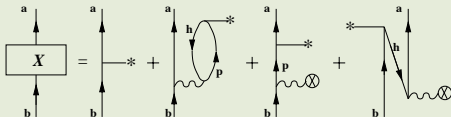
$$\begin{aligned}\hat{\Theta}(\epsilon) &= P\Theta P + P\Theta Q \frac{1}{\epsilon - QHQ} QH_1 P \\ \hat{\Theta}(\epsilon_1; \epsilon_2) &= PH_1 Q \frac{1}{\epsilon_1 - QHQ} \times \\ &\quad Q\Theta Q \frac{1}{\epsilon_2 - QHQ} QH_1 P\end{aligned}$$

$$\begin{aligned}\hat{\Theta}_m &= \frac{1}{m!} \left. \frac{d^m \hat{\Theta}(\epsilon)}{d\epsilon^m} \right|_{\epsilon=\epsilon_0} \\ \hat{\Theta}_{nm} &= \frac{1}{n!m!} \left. \frac{d^n}{d\epsilon_1^n} \frac{d^m}{d\epsilon_2^m} \hat{\Theta}(\epsilon_1; \epsilon_2) \right|_{\epsilon_{1,2}=\epsilon_0}\end{aligned}$$

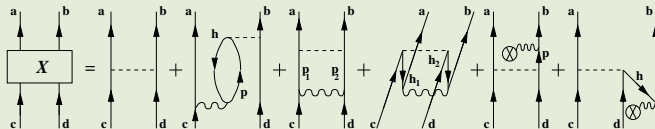
The shell-model effective operators

We arrest the χ series at χ_2 term, and then expand $\hat{\Theta}$ perturbatively:

One-body operator



Two-body operator



- J. D. Holt and J. Engel, *Phys. Rev. C* **87**, 064315 (2013).
- L.C., L. De Angelis, T. Fukui, A. Gargano, and N. Itaco, *Phys. Rev. C* **95**, 064324 (2017).
- L.C., L. De Angelis, T. Fukui, A. Gargano, and N. Itaco (2019), *arXiv:1812.04292v2[nucl-th]*, in press in *Phys. Rev. C*.

Nuclear models and predictive power

Nuclear model



Accurate reproduction
of experimental data



Predictive power

Realistic SM calculations for ^{48}Ca , ^{76}Ge , ^{82}Se , ^{130}Te , and ^{136}Xe



Check our approach calculating GT strengths and $2\nu\beta\beta$ -decay

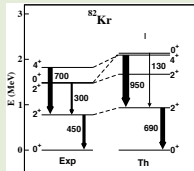
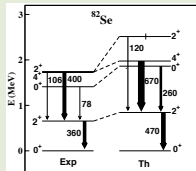
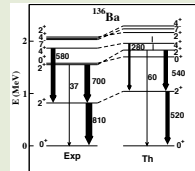
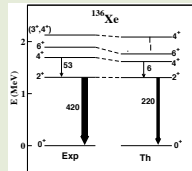
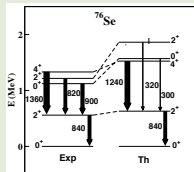
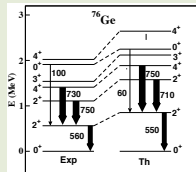
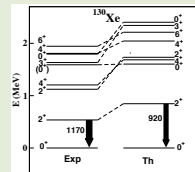
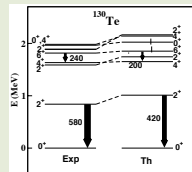
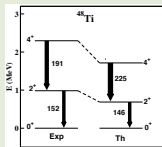
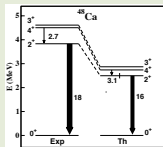
$$\left[T_{1/2}^{2\nu}\right]^{-1} = G^{2\nu} \left|M_{\text{GT}}^{2\nu}\right|^2$$

where

$$M_{2\nu}^{\text{GT}} = \sum_n \frac{\langle 0_f^+ || \vec{\sigma}\tau^- || 1_n^+ \rangle \langle 1_n^+ || \vec{\sigma}\tau^- || 0_i^+ \rangle}{E_n + E_0}$$

- ^{48}Ca : four proton and neutron orbitals outside doubly-closed ^{40}Ca
 $0f_{7/2}, 0f_{5/2}, 1p_{3/2}, 1p_{1/2}$
- $^{76}\text{Ge}, ^{82}\text{Se}$: four proton and neutron orbitals outside doubly-closed ^{56}Ni
 $0f_{5/2}, 1p_{3/2}, 1p_{1/2}, 0g_{9/2}$
- $^{130}\text{Te}, ^{136}\text{Xe}$: five proton and neutron orbitals outside doubly-closed ^{100}Sn
 $0g_{7/2}, 1d_{5/2}, 1d_{3/2}, 2s_{1/2}, 0h_{11/2}$

Spectroscopic properties



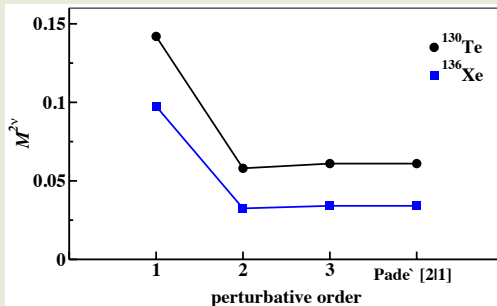
Perturbative properties of the GT effective operator

Convergence with respect the number of intermediate states

Selection rules of the GT operator make the convergence of the effective one with respect to N_{\max} very fast.

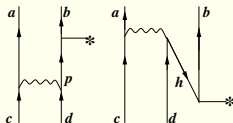
The third decimal digit value of $M_{\text{GT}}^{2\nu}$, calculated with effective operator at third order, does not change from $N_{\max} = 12$ on.

Order-by-order convergence

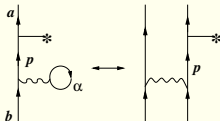


The blocking effect

Blocking (Pauli) effect: the filling of the model-space orbitals by the valence nucleons affects the calculation of the effective GT operator:

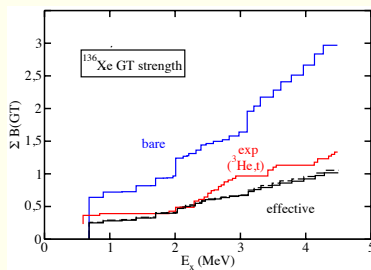
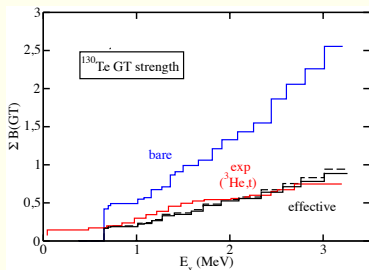
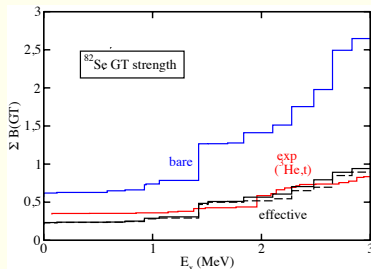
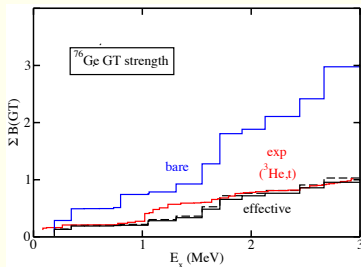


Many-body correlations need to be taken into account: we calculate two-body correlations diagram and sum over one of the incoming/outcoming nucleons



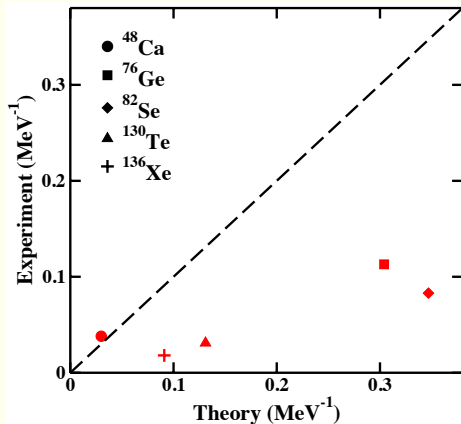
We then obtain a **density-dependent** one-body GT effective operator
The calculated $M_{GT}^{2\nu}$ are affected less than 5%

GT- running sums



Dashed lines: calculations accounting for the **blocking effect**

$2\nu\beta\beta$ nuclear matrix elements

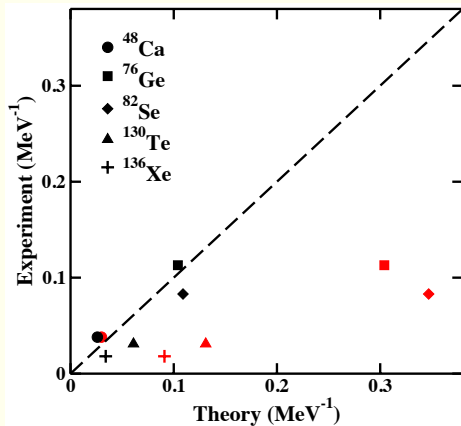


Red dots: bare GT operator

Decay	Expt.	Bare
$^{48}\text{Ca} \rightarrow ^{48}\text{Ti}$	0.038 ± 0.003	0.030
$^{76}\text{Ge} \rightarrow ^{76}\text{Se}$	0.113 ± 0.006	0.304
$^{82}\text{Se} \rightarrow ^{82}\text{Kr}$	0.083 ± 0.004	0.347
$^{130}\text{Te} \rightarrow ^{130}\text{Xe}$	0.031 ± 0.004	0.131
$^{136}\text{Xe} \rightarrow ^{136}\text{Ba}$	0.0181 ± 0.0007	0.0910

Experimental data from [A. S. Barabash, Nucl. Phys. A 935, 52 \(2015\)](#)

$2\nu\beta\beta$ nuclear matrix elements



Red dots: bare GT operator
Black triangles: effective GT operator

Decay	Expt.	Eff.
$^{48}\text{Ca} \rightarrow ^{48}\text{Ti}$	0.038 ± 0.003	0.026
$^{76}\text{Ge} \rightarrow ^{76}\text{Se}$	0.113 ± 0.006	0.104
$^{82}\text{Se} \rightarrow ^{82}\text{Kr}$	0.083 ± 0.004	0.109
$^{130}\text{Te} \rightarrow ^{130}\text{Xe}$	0.031 ± 0.004	0.061
$^{136}\text{Xe} \rightarrow ^{136}\text{Ba}$	0.0181 ± 0.0007	0.0341

Experimental data from [A. S. Barabash, Nucl. Phys. A 935, 52 \(2015\)](#)

- [L.C., L. De Angelis, T. Fukui, A. Gargano, and N. Itaco, Phys. Rev. C **95**, 064324 \(2017\).](#)
- [L.C., L. De Angelis, T. Fukui, A. Gargano, and N. Itaco \(2019\), arXiv:1812.04292v2\[nucl-th\], in press in Phys. Rev. C.](#)

The calculation of $M^{0\nu}$

The matrix elements $M_\alpha^{0\nu}$ are defined as follows:

$$M_\alpha^{0\nu} = \sum_k \sum_{j_p j_{p'} j_n j_{n'} J_\pi} \langle f | a_p^\dagger a_n | k \rangle \langle k | a_{p'}^\dagger a_{n'} | i \rangle \langle j_n j_{n'}; J^\pi | \tau_1^- \tau_2^- O_{12}^\alpha | j_p j_{p'}; J^\pi \rangle$$

with $\alpha = (GT, F, T)$

$$O_{12}^{GT} = \vec{\sigma}_1 \cdot \vec{\sigma}_2 H_{GT}(r)$$

$$O_{12}^F = H_F(r)$$

$$O_{12}^T = [3(\vec{\sigma}_1 \cdot \hat{r})(\vec{\sigma}_1 \cdot \hat{r}) - \vec{\sigma}_1 \cdot \vec{\sigma}_2] H_T(r)$$

H_α depends on the energy of the initial, final, and intermediate states:

$$H_\alpha(r) = \frac{2R}{\pi} \int_0^\infty \frac{j_\alpha(qr) h_\alpha(q^2) q dq}{q + E_k - (E_i + E_f)/2}$$

Actually, because of the computational complexity, the energies of the intermediate states are replaced by an average value:

$$E_k - (E_i + E_f)/2 \rightarrow \langle E \rangle$$

$$\sum_k \langle f | a_p^\dagger a_n | k \rangle \langle k | a_{p'}^\dagger a_{n'} | i \rangle = \langle f | a_p^\dagger a_n a_{p'}^\dagger a_{n'} | i \rangle$$

The closure approximation

Consequently, the expression of the neutrino potentials becomes:

$$H_{\alpha}(r) = \frac{2R}{\pi} \int_0^{\infty} \frac{j_{\alpha}(qr) h_{\alpha}(q^2) q dq}{q + \langle E \rangle}$$

The matrix elements $M_{\alpha}^{0\nu}$ are then defined, within the **closure approximation**, as follows:

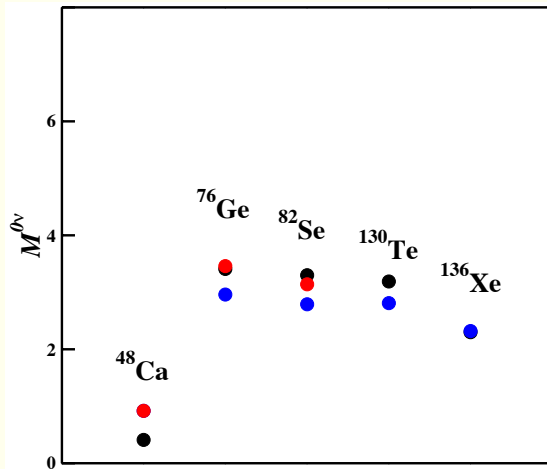
$$M_{\alpha}^{0\nu} = \sum_{j_n j_{n'} j_p j_{p'} J_{\pi}} TBTD(j_n j_{n'}, j_p j_{p'}; J_i J_f) \langle j_n j_{n'}; J^{\pi} | \tau_1^{-} \tau_2^{-} O_{12}^{\alpha} | j_p j_{p'}; J^{\pi} \rangle$$

The **TBTD** are the **two-body transition-density** matrix elements, and the Gamow-Teller (**GT**), Fermi (**F**), and tensor (**T**) operators:

The closure approximation works since $q \approx 100\text{-}200 \text{ MeV}$, while model-space excitation energies $E_{\text{exc}} \approx 10 \text{ MeV}$

Sen'kov and Horoi (Phys. Rev. C **88**, 064312 (2013)) have evaluated the non-closure vs closure approximation within **10%**

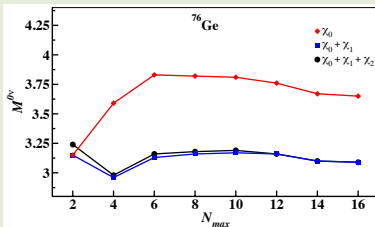
Shell model calculations of $M^{0\nu}$



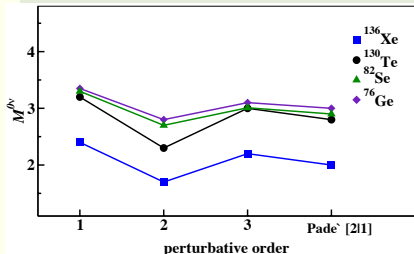
- Blue dots: Madrid-Strasbourg group, bare $0\nu\beta\beta$ operator
- Red dots: Horoi *et al.*, bare $0\nu\beta\beta$ operator
- Black dots: RSM, bare $0\nu\beta\beta$ operator

Perturbative properties of the 00ν effective operator

Convergence with respect the number of intermediate states



Order-by-order convergence



The perturbative behavior is not satisfactory as for the $\text{single-}\beta$ decay operator: $\text{third-order contribution}$ is rather large compared to the second order one

$0\nu\beta\beta$ decay: short-range correlations

The issue of the SRC for the calculation of $M^{0\nu}$ is framed within the approach of the renormalization of the NN potential

$V_{\text{low-k}}$: the configurations of $V_{NN}(k, k')$ are restricted to those with $k, k' < k_{\text{cutoff}} = \Lambda$

The $V_{\text{low-k}}$ is obtained *via* a unitary transformation Ω

$$\mathcal{H}_{\text{low-k}} = T + V_{\text{low-k}}(k, k') = \Omega^{-1} H_{NN}(k, k') \Omega = T + \Omega^{-1} V_{NN}(k, k') \Omega$$

Consistently, we transform the $0\nu\beta\beta$ operator by way of the same similarity transformation Ω

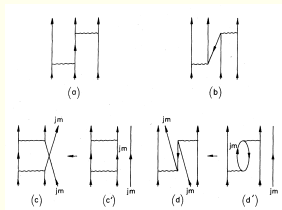
$$O_{\text{low-k}} = \Omega^{-1} O(k, k') \Omega$$

The SRC affects less than 5%.

For ^{76}Ge : $M_{\text{bare}}^{0\nu} = 3.41 \rightarrow M_{\text{low-k}}^{0\nu} = 3.29$

The blocking effect

Blocking (Pauli) effect: as for the one-body operators, the filling of the model-space orbitals by the valence nucleons affects the effective $0\nu\beta\beta$ operator:



Many-body correlations are taken into account by calculating three-body correlations diagrams and summing over one of the incoming/outcoming nucleons



We obtain a **density-dependent** two-body $0\nu\beta\beta$ effective operator

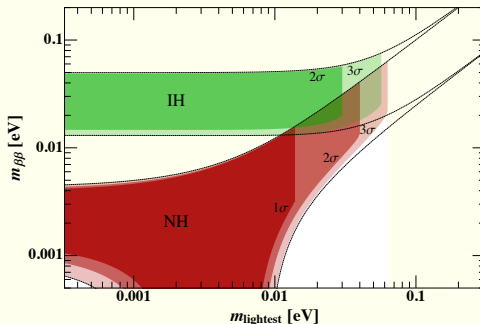
The calculation of $M^{0\nu}$: results

Decay	$M_{\text{bare}}^{0\nu}$	$M_{\text{src}}^{0\nu}$	$M_{\text{eff}}^{0\nu}$	$M_{\text{eff}+3b}^{0\nu}$
$^{48}\text{Ca} \rightarrow ^{48}\text{Ti}$	0.53	0.53	0.30	0.30
$^{76}\text{Ge} \rightarrow ^{76}\text{Se}$	3.41	3.29	3.02	2.66
$^{82}\text{Se} \rightarrow ^{82}\text{Kr}$	3.30	3.25	2.95	2.73
$^{130}\text{Te} \rightarrow ^{130}\text{Xe}$	3.19	3.14	2.97	3.19
$^{136}\text{Xe} \rightarrow ^{136}\text{Ba}$	2.30	2.30	2.17	2.34

The experimental bound on $^{136}\text{Xe} \rightarrow ^{136}\text{Ba}$ process from KamLAND-Zen ($T_{1/2}^{0\nu} > 1.1 \times 10^{26} \text{yr}$) corresponds to our upper bound of neutrino effective mass $\langle m_\nu \rangle < 0.11 \text{ eV}$

	$^{48}\text{Ca} \rightarrow ^{48}\text{Ti}$	$^{76}\text{Ge} \rightarrow ^{76}\text{Se}$	$^{82}\text{Se} \rightarrow ^{82}\text{Kr}$	$^{130}\text{Te} \rightarrow ^{130}\text{Xe}$
$T_{1/2}^{0\nu} \text{ (in yr)}$	$> 3.7 \times 10^{27}$	$> 5 \times 10^{26}$	$> 1.1 \times 10^{26}$	$> 5.8 \times 10^{25}$

The calculation of $M^{0\nu}$: results



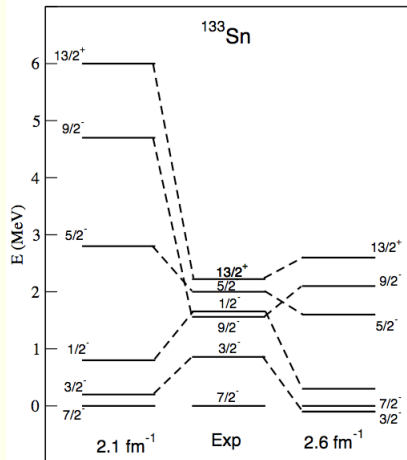
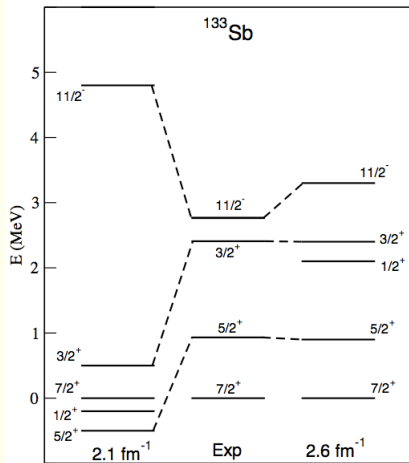
To rule out the Inverted Hierarchy of neutrino mass spectra, the upper bound of neutrino effective mass should be $\langle m_\nu \rangle < 0.01 \text{ eV}$.

We could then evaluate the lower bound of the half lives of the decay processes, accordingly to our calculated $M^{0\nu}$

	$^{76}\text{Ge} \rightarrow ^{76}\text{Se}$	$^{82}\text{Se} \rightarrow ^{82}\text{Kr}$	$^{130}\text{Te} \rightarrow ^{130}\text{Xe}$	$^{136}\text{Xe} \rightarrow ^{136}\text{Ba}$
$T_{1/2}^{0\nu}$ (in yr)	$> 6 \times 10^{28}$	$> 1 \times 10^{28}$	$> 7 \times 10^{27}$	$> 1 \times 10^{28}$

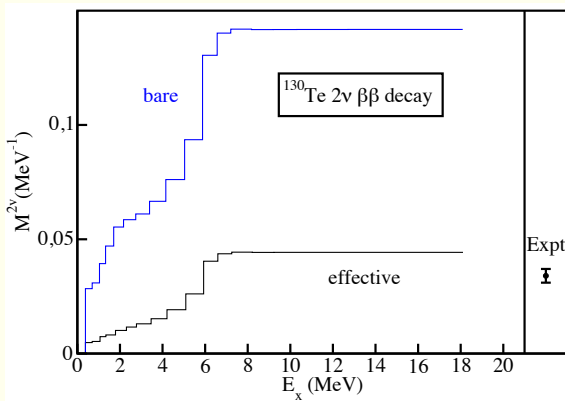
- Calculation of the effective $0\nu\beta\beta$ beyond the closure approximation
- Derivation of H_{eff} from chiral two- and three-body potentials
- Evaluation of the effects of **chiral two-body currents** (for both $2\nu\beta\beta$ and $0\nu\beta\beta$ decays)

The choice of the cutoff $\Lambda = 2.6 \text{ fm}^{-1}$



L. C., A. Gargano, and N. Itaco, JPS Conf. Proc. 6, 020046 (2015)

$^{130}\text{Te} \rightarrow ^{130}\text{Xe}$: convergence with respect ^{130}Cs $J^\pi = 1^+$ intermediate states



The blocking effect

Gamow-Teller two-body matrix elements

Decay	$j_a j_b j_c j_d; J = 0^+$	ladder	3b (a)	3p-1h	3b (b)
$^{48}\text{Ca} \rightarrow ^{48}\text{Ti}$	$0f_{7/2}0f_{7/2}0f_{7/2}0f_{7/2}$	-0.334	0.004	0.260	-0.017
$^{76}\text{Ge} \rightarrow ^{76}\text{Se}$	$0g_{9/2}0g_{9/2}0f_{5/2}0f_{5/2}$	0.154	-0.241	-1.078	0.234
	$0g_{9/2}0g_{9/2}1p_{3/2}1p_{3/2}$	0.185	-0.246	-0.214	0.048
$^{82}\text{Se} \rightarrow ^{82}\text{Kr}$	$0g_{9/2}0g_{9/2}0f_{5/2}0f_{5/2}$	0.157	-0.337	-1.096	0.335
	$0g_{9/2}0g_{9/2}1p_{3/2}1p_{3/2}$	0.189	-0.263	-0.219	0.058
$^{130}\text{Te} \rightarrow ^{130}\text{Xe}$	$0h_{11/2}0h_{11/2}0g_{7/2}0g_{7/2}$	0.171	-0.202	-0.948	0.297
$^{136}\text{Xe} \rightarrow ^{136}\text{Ba}$	$0h_{11/2}0h_{11/2}0g_{7/2}0g_{7/2}$	0.178	-0.264	-0.997	0.381

As we expect:

- 3-body (a) diagram reduces the contribution of the 2-body ladder diagram
- 3-body (b) diagram reduces the contribution of the 2-body 3p-1h (core polarization) diagram